Available online at www.sciencedirect.com
ScienceDirect
Developmental Biology 307 (2007) 258–271
DEVELOPMENTAL BIOLOGY
www.elsevier.com/locate/ydbio

Foxi3 transcription factors and Notch signaling control the formation of skin ionocytes from epidermal precursors of the zebrafish embryo

Martina Jänicke [a], Thomas J. Carney [a], Matthias Hammerschmidt [a,b,*]

[a] *Max-Planck-Institute of Immunobiology, Stuebeweg 51, D-79108 Freiburg, Germany*
[b] *Institute for Developmental Biology, University of Cologne, Gyrhofstrasse 17, D-50923 Cologne, Germany*

Received for publication 3 January 2007; revised 30 March 2007; accepted 27 April 2007
Available online 3 May 2007

Abstract

Ionocytes are specialized epithelial cell types involved in the maintenance of osmotic homeostasis. In amniotes, they are present in the renal system, while in water-living embryos of lower vertebrates additional ionocytes are found in the skin. Thus far, relatively little has been known about the mechanisms of ionocyte development. Here we demonstrate that skin ionocytes of zebrafish embryos derive from the same precursor cells as keratinocytes. Carrying out various combinations of gain- and loss-of-function studies, we show that the segregation of ionocytes from the epidermal epithelium is governed by an interplay between Notch signaling and two Forkhead-box transcription factors, Foxi3a and Foxi3b. The two *foxi3* genes are expressed in ionocyte precursors and are required both for ionocyte-specific expression of the Notch ligand Jagged2a, and for ionocyte differentiation, characterized by the production of particular ATPases. Ionocytic Notch ligands, in turn, signal to neighboring cells, where activated Notch1 leads to a repression of *foxi3* expression, allowing those cells to become keratinocytes. A model for ionocyte versus keratinocyte development will be presented, postulating additional thus far unidentified pro-ionocyte factors.

Keywords: Ionocytes; Skin; Foxi3; Notch; p63; Zebrafish; Osmoregulation

Introduction

Ion transporting epithelia are involved in the maintenance of osmotic homeostasis by regulating ion exchange and acid–base balance of the body fluids of an organism. A specialized cell type, called ionocyte or mitochondria-rich cell, selectively transports ions against a concentration gradient. These cells can be found in a variety of organs including the kidneys of amniotes, the urinary system and the skin of amphibia as well as in the gills and the skin of teleost fish (reviewed in Brown and Breton, 1996). The main characteristics of ionocytes are a high abundance of mitochondria and a large number of apical microvilli that highly express ATPases, mainly Na^+/K^+-ATPases and V-type H^+-ATPases (Brown and Breton, 1996).

Ionocytes in the gills of teleost fish have been extensively studied because they are easily accessible for morphological and physiological analysis (Claiborne et al., 2002; Perry et al., 2003) (reviewed in Boisen et al., 2003; Goss et al., 1992). Teleost freshwater fish are hyperosmotic to their environment and are therefore submitted to a constant passive influx of water as well as to a diffusive loss of ions, mainly Na^+, K^+, Cl^- and Ca^{2+}. The production of hypotonic urine and the active uptake of ions from the environment compensate for this loss and maintain osmotic homeostasis. Prior to the development of functional gills, ionocytes in the skin form the main site of osmoregulation in the fish larvae. During later development a shift in the distribution of ionocytes has been observed from the skin to the gills in most species analyzed (reviewed in Varsamos et al., 2005).

In the skin of zebrafish larvae two distinct types of ionocytes have been described (Lin et al., 2006). At 24 h post-fertilization (hpf), Na^+-pump-rich cells (NaR cells) are spread as single cells throughout the skin of the trunk, the yolk sac and the yolk sac extension. This cell type is characterized by high expression of Na^+/K^+-ATPase. A subset of these NaR cells also contains an epithelial Ca^{2+}-channel, and numbers of this cell type are increased upon incubation in low-Ca^{2+} media (Pan et al., 2005).

* Corresponding author. Max-Planck-Institute of Immunobiology, Stuebeweg 51, D-79108 Freiburg, Germany. Fax: +49 761 5108 744.
E-mail address: hammerschmid@immunbio.mpg.de (M. Hammerschmidt).

0012-1606/$ - see front matter © 2007 Elsevier Inc. All rights reserved.
doi:10.1016/j.ydbio.2007.04.044

A second type of ionocytes, called H^+-pump-rich cells (HR cells), is characterized by high expression of V-type H^+-pump ATPase and its distribution is restricted to the yolk sac and the yolk sac extension. These cells generate a strong outward proton flux that creates an electrical gradient for the uptake of Na^+ ions (Lin et al., 2006). Recently is has been shown that HR cells are the main cell type for the absorbance of Na^+ ions (Esaki et al., 2006).

Though numerous studies have investigated the physiology underlying ion transport in fish, the genetic mechanisms regulating the development of ionocytes are largely unknown. During the first days of development, the zebrafish skin consists of two layers of epithelial cells, the basal layer, which is derived from the non-neural/ventral embryonic ectoderm, and the external layer of cells, the periderm, which is a derivative of the embryonic enveloping layer (EVL) (Kimmel et al., 1990; Le Guellec et al., 2004). The transcription factor ΔNp63, a relative of the tumor suppressor protein p53, has been shown to be crucial for the proliferation and development of keratinocytes in the basal epidermal layer (Bakkers et al., 2002; Lee and Kimelman, 2002). However, little is known about the origin of the ionocytes of the skin and the factors involved in their differentiation. A recent study describes that antisense-mediated knockdown of a forkhead box transcription factor, *foxi3a*, leads to a reduction in the number of HR cells (Esaki et al., 2006).

Here we have analyzed the embryonic origin of zebrafish skin ionocytes. In addition, we have carried out further analyses of the genetic control of ionocyte development. We show that ionocytes and keratinocytes derive from the same progenitor cells within the ventral ectoderm. The *forkhead* box genes *foxi3a* and *foxi3b*, which start to be expressed in a subset of the ΔNp63-positive keratinocyte/ionocyte precursors during early segmentation stages, are absolutely essential for ionocyte formation, while ΔNp63 seems to be largely unimportant for both ionocyte proliferation and specification. Ectopic *foxi3* expression causes massive ionocyte formation in the normally ionocyte-free epidermis of the head region, while ionocyte density in their natural domains in trunk and tail remains largely unaltered. Here, ionocyte density is regulated by Notch signaling, constituting a system of lateral inhibition as used for singling out of particular cell types during many different processes of vertebrate and invertebrate development (reviewed in Lewis, 1998).

Materials and methods

Zebrafish strains

Ionocytes were analyzed in the *mib*^{ta52b} (Itoh et al., 2003), *des*^{tp37a} (Gray et al., 2001), *bea*^{tm98} (Julich et al., 2005) and *aei*^{tr233} (Holley et al., 2000) mutant strains. Lineage tracing experiments were performed with the tg(β-*actin:mGFP*) transgenic line (Cooper et al., 2005). For heat shock experiments carriers of the *hsp70:Gal4* transgene were mated to carriers of the *UAS:notch1a-icd* transgene (Scheer and Campos-Ortega, 1999).

Labeling procedures

Whole-mount in situ hybridizations and immunostainings were performed as previously described (Hammerschmidt et al., 1996). ΔNp63 protein was detected with the mouse anti-p63 antibody 4A4 (Santa Cruz), as previously described (Bakkers et al., 2005). For in situ hybridizations, the following riboprobes were used: *foxi3a* and *foxi3b* (Solomon et al., 2003), collagen type I alpha1 (*col1a1*) (Fisher et al., 2003), *deltaA-D* (Haddon et al., 1998), *atp1b1b* (clone IRBOp991B031D, RZPD, Germany, linearized with *Sal*I and transcribed with T3 RNA polymerase), *atp6v1al* (clone IRBOp991H0925D, RZPD, Germany, probe synthesis by PCR following the protocol on ZFIN.org) and *jagged2b* (clone MDR1738-8974408, OpenBiosystems, USA). For the *jagged1a*, *jagged1b* and *jagged2a* riboprobes, fragment were amplified from cDNA using the primers TAA TAC GAC TCA CTA TAG GGA GGC AGA CAT AAA GAA ACA CC (jag1a-sense), TAA TAC GAC TCA CTA TAG GGA GGC CAA TAC TAA TGC CGA T (jag1a-antisense), TAA TAC GAC TCA CTA TAG GGA GGG CTG TGT TGC CCC TG (jag1b-sense), TAA TAC GAC TCA CTA TAG GGA GGT GTG AAT ACT TCT GTA C (jag1b-antisense), TAA TAC GAC TCA CTA TAG GGA GGG ATG AGC AGG ACG AG (jag2a-sense) and TAA TAC GAC TCA CTA TAG GGA GGG TAA GGG AAG GGA TTG (jag2a-antisense) and ligated into pGEMTeasy. The vector was linearized with *Hin*dIII and transcribed with T7 RNA polymerase. For single in situ hybridizations, probes were labeled with digoxygenin (Roche). In addition, for double in situ hybridizations, riboprobes for *foxi3a*, *foxi3b* and *atp6v1al* were labeled with fluorescein (Roche).

For fluorescent in situ hybridizations, the digoxygenin-labeled probe was developed using FastRed tablets (Sigma) according to the manufacturer's instructions. Fluorescent double in situ hybridizations were performed basically as described (Clay and Ramkrishnan, 2005). The digoxygenin-labeled probe was detected first, using FastRed substrate. For detection of the fluorescein-labeled probe, embryos were briefly washed in PBST, re-blocked for 1 h at room temperature and incubated with a rabbit anti-fluorescein antibody (Molecular Probes) at 4 °C over night. Afterwards, embryos were extensively washed in PBST, re-blocked, incubated with secondary HRP-conjugated anti-rabbit antibody (provided with the TSA kit, Molecular Probes) and processed with the Tyramid Signal Amplification Kit #12 (Molecular Probes) according to the manufacturer's instructions. Photographs were taken with a Zeiss LSM510 META confocal microscope.

Morpholino and synthetic mRNA injections

Antisense morpholinos (MO) were purchased from GeneTools and injected into one- to two-cell stage embryos as described previously (Nasevicius and Ekker, 2000). The ΔNp63-MO was as previously described (Bakkers et al., 2002). MOs against *jagged1a*, *jagged1b* and *jagged2a* were as described previously (Lorent et al., 2004)). Sequences of foxi3-MOs were GGA TGT CAT TGC TCG ATC CTG AGG G (*foxi3a*); GAC TGT GGA ACA AAT GAT GTC ATG C (*foxi3b*). The sequence of the foxi3a-MO differs from the one used by Esaki et al. (2006). Sequences for Jagged2b-MOs targeting the splice donor of intron C or the splice acceptor of intron R, respectively, were TCA TTA CTT ACT ACT CTC TGT AAT T (Jag2b MO1) and GTC GTC AAC ATC TGA AAA CAG AAT C (Jag2b MO2). Jagged morpholinos were injected at the following concentrations: 0.025 mM (Jag1a), 0.2 mM (Jag1b, Jag2a, Jag2b) and 0.1 mM (Jag2b MO1+2). For quadruple injections, morpholinos were diluted to final concentrations of 6.25 μM (Jag1a), 50 μM (Jag1b, Jag2a) and 25 μM (Jag2b MO1+2).

The full-length open reading frames of *foxi3a* and *foxi3b* were amplified from 24 hpf cDNA using Advantage Taq DNA Polymerase (Clontech) and ligated into the *Xho*I and *Xba*I sites in pCS2+. PCR primers used were GCT AGC TCG AGA TGA CAT CAT TTG TTC CAC AGT C (Foxi3a-sense), GCT CTA GAT TAC ACC TCA GAT CCC TCC C (Foxi3a-antisense), GCT AGC TCG AGA TGA CAT CCT ACG AGT CTC AAG G (Foxi3b-sense) and GCT CTA GAC TAC ACC TCT GTG CCT TCC C (Foxi3b-antisense). Following plasmid linearization with *Acc*651, capped RNA was synthesized using the SP6 polymerase message machine kit (Ambion, USA). Synthesis of *ΔNp63α* mRNA was done as previously described (Bakkers et al., 2002). Capped mRNA was injected into one-cell stage embryos at a concentration of 5 ng/μl (*foxi3a*, *foxi3b*) or 20 ng/μl (*ΔNp63α*).

Heat shock experiments

For heat shock experiments heterozygous *hsp70:Gal4* and *UAS:notch1a-icd* fish were crossed and embryos raised at 28 °C until the desired stages. Heat shocks were performed by replacing the embryo medium with medium pre-

warmed to 40 °C, followed by incubation at 40 °C for 30 min. Then, embryo medium was replaced by medium at 28 °C and embryos were incubated at 28 °C. Fish were fixed at 24 hpf and in situ hybridizations were performed as described.

Lineage tracing experiments

At shield stage (6 hpf), single cells were homochronically transplanted from the ventral ectoderm of a *β-actin:mGFP* transgenic embryo (Cooper et al., 2005) into the same region of a non-transgenic recipient. Recipients were fixed at 24 hpf, followed by fluorescent in situ hybridization for *atp1b1b* and *atp6v1al*, as described above, and fluorescent immunolabeling of keratinocytes (primary mouse-anti-p63 antibody 4A4 (Santa Cruz) and anti-mouse-Alexa647; Molecular Probes) and of the descendants of transplanted cells (primary rabbit anti-GFP antibody and secondary anti-rabbit-Alexa488 antibody; Molecular Probes).

Results

foxi3a and foxi3b are expressed in two distinct types of epidermal ionocytes and display transient co-expression with the keratinocyte marker ΔNp63

Via cytochemical and electrophysiological approaches, two distinct ionocyte cell types can be distinguished in the skin of zebrafish embryos (Lin et al., 2006). In the present study, expression of a Na^+/K^+-ATPase subunit, *atp1b1b*, was used as a marker for NaR cells, while expression of an H^+-pump subunit, *atp6v1al*, was used to label HR cells. At 24 h post-fertilization (hpf), *atp1b1b* and *atp6v1al* were expressed in a punctate but mutually exclusive manner. Cells expressing *atp1b1b* were present in both ventral and dorsal regions of trunk and tail, whereas *atp6v1al*-positive cells were restricted to ventral regions (Fig. 1A).

Performing in situ hybridizations at different developmental stages, we found *atp1b1* expression to be initiated around the 11-somite, and *atp6v1al* around the 15-somite stage (data not shown), consistent with online data published in Zfin (Thisse et al., 2001; http://zfin.org). To be able to investigate the genetic control of ionocyte development, we searched for genes expressed in ionocyte precursor cells prior to *ATPases*. The expression of two *forkhead* box genes, *foxi3a* and *foxi3b*, was described in single cells covering the yolk of the embryo from 10 hpf onwards (tailbud, 1-somite stage) (Esaki et al., 2006; Solomon et al., 2003). These cells were initially annotated as mucous cells. However, carrying out double fluorescent in situ hybridization, we found that both *foxi3a* and *foxi3b* are co-expressed with *atp1b1b* at 24 hpf (Figs. 1B, C). In addition *foxi3a* expression was recently reported in HR cells (Esaki et al., 2006). Interestingly, at 24 hpf, *foxi3a* and *foxi3b* were only expressed in a subset of the *atp1b1*-positive cells, suggesting that their expression might cease in fully differentiated ionocytes (see also below). Together, these data identify *foxi3a* and *foxi3b* as markers for ionocyte precursors.

Over the first 5 days of development, ionocytes are distributed in a punctate pattern throughout the epidermis of the zebrafish embryo. During this time the epidermis consists of two cell layers that are separated from the dermis by a basement membrane (Le Guellec et al., 2004). Cells of the basal layer of

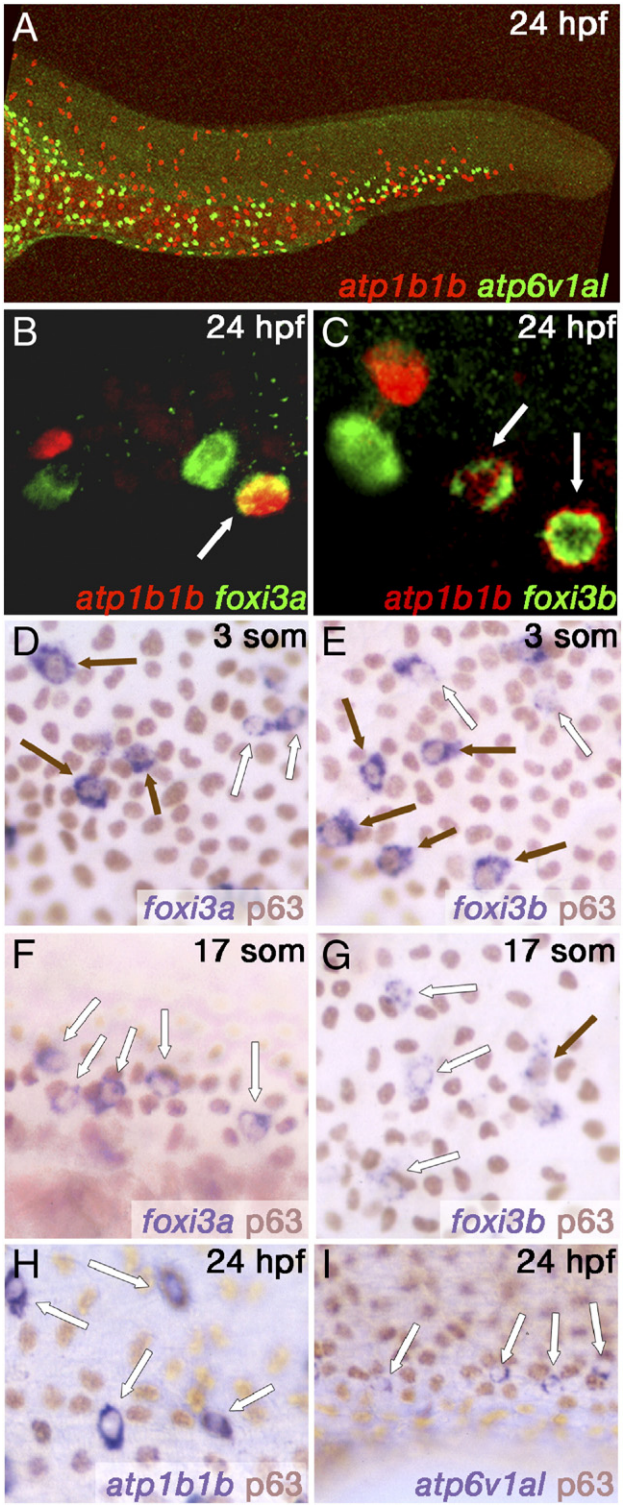

Fig. 1. Ionocyte precursors display temporal expression of *foxi3a*, *foxi3b* and Δ*Np63*. Panels A–C show double-fluorescent whole-mount in situ hybridizations of wild-type embryos at 24 hpf, with probes indicated in the lower right corners. (B, C) Double-positive cells are indicated by arrows. Panels D–I show whole-mount in situ hyridizations of wild-type embryos, followed by antibody staining for p63. Black arrows highlight p63-positive, white arrows p63-negative ionocyte precursors. Probes are indicated in lower right corners, stages of embryos in top right corners. (A) A lateral view of the trunk with anterior to the left, (B–I) high magnification views of cells on the yolk sac.

the epidermis are characterized by the expression of Δ*Np63*, encoding a transcription factor important for the proliferation of keratinocyte precursor cells, but most likely dispensable for keratinocyte differentiation (Bakkers et al., 2002; Lee and Kimelman, 2002). Expression of Δ*Np63* in keratinocyte precursor cells starts during mid gastrula stages (8 hpf; Bakkers et al., 2005, 2002), while expression of *foxi3a* and *foxi3b* is initiated approximately 2 h later (10 hpf). Performing *foxi3* in situ hybridizations in combination with anti-p63 immunostainings, we found that both *foxi3a* and *foxi3b* are temporarily co-expressed with Δ*Np63* (Figs. 1D–G). At the 3-somite stage (11 hpf), approximately 90% of the *foxi3*-positive cells contain nuclear ΔNp63 protein (Figs. 1D, E). However, the ratio of co-expressing cells progressively decreases during further development. At the 11-somite stage, ΔNp63 protein is only found in approximately 20% of the *foxi3*-positive cells (Figs. 1F, G). This is in contrast to the *foxi3*-negative epidermal cells, which remain ΔNp63-positive and give rise to keratinocytes. These data indicate that ionocyte precursor cells transiently express Δ*Np63*, which becomes downregulated as ionocyte specification progresses. Consistent with this notion, more advanced ionocytes, characterized by the expression of *atp1b1* or *atp6v1al*, lack ΔNp63 protein at 24 hpf (Figs. 2H, I). The co-existence of Δ*Np63*-positive and Δ*Np63*-negative Foxi3 cells during segmentation stages (Figs. 1D–G) and of *foxi3*-positive and *foxi3*-negative ATPase cells at 24 hpf (Figs. 1B, C) further indicates the presence of differently advanced ionocytes within one and the same tissue, suggesting that the onset of ionocyte specification can vary from cell to cell (see also Discussion).

Ionocytes and keratinocytes are derived from the same progenitor cells in the ventral ectoderm

The transient co-expression of *p63* and *foxi3* in ionocyte precursors strongly suggests that keratinocytes and ionocytes

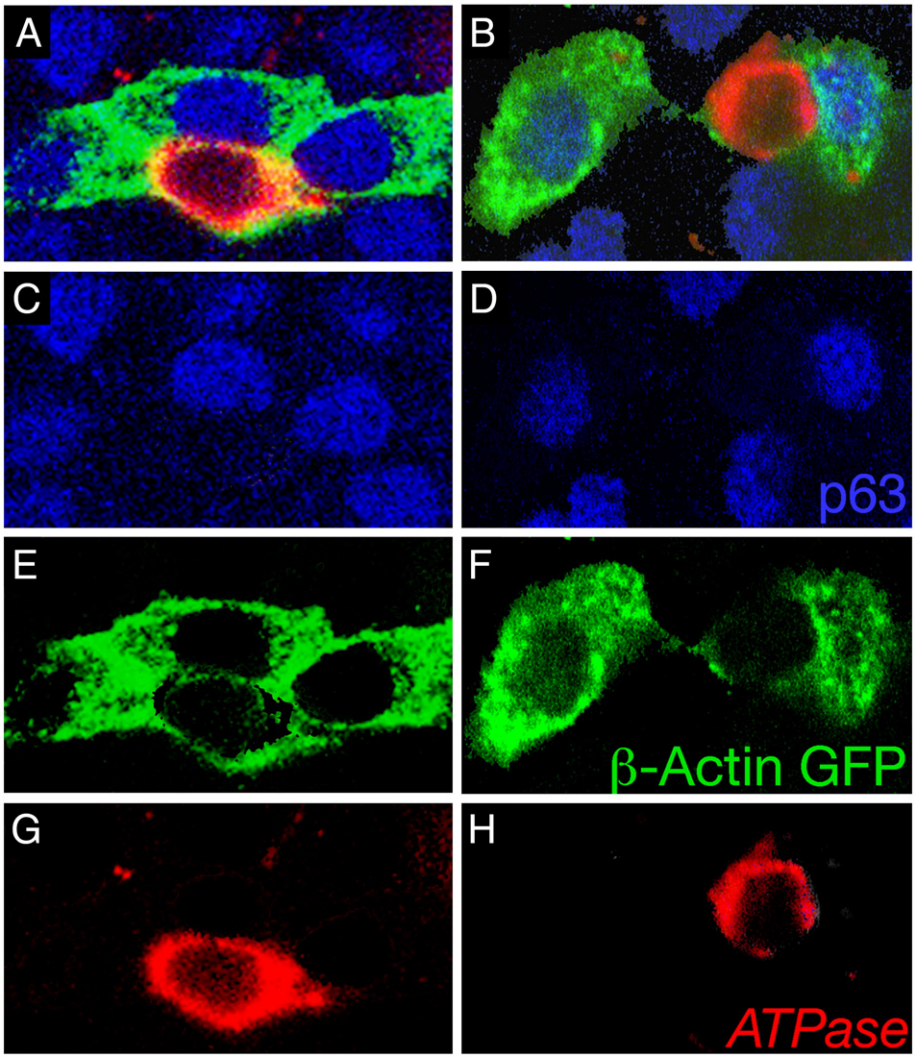

Fig. 2. Ionocytes and keratinocytes derive from common precursor cells from the ventral ectoderm. High magnification views of the epidermis of 24 hpf wild-type embryos after homotopic and homochronic transplantation of single β-*actin:mGFP* transgenic cells into the ventral ectoderm at 6 hpf (shield stage). Panels A and B show the merge of panels C, E, G or D, F, H, respectively. Panels C and D show anti-p63 immunostainings of keratinocytes, panels E and F anti-GFP immunolabeling of cell clones deriving from the transplanted ventral ectodermal cells and panels G and H fluorescent *atp1b1*/*atp6v1al* in situ hybridizations marking ionocytes.

have the same embryonic origin. To obtain direct evidence for this notion, we performed cell-lineage experiments, tracing single labeled precursor cells over time. According to fate mapping studies, ΔNp63-positive keratinocytes of the basal epidermal layer derive from the non-neural, ventral ectoderm of early zebrafish gastrula (Kimmel et al., 1990). We transplanted single ventral ectodermal cells from *β-actin:mGFP* transgenic hosts into the same region of unlabeled recipients at shield stage (6 hpf) and determined the nature of their descendants at 24 hpf via co-stainings for the ionocyte *ATPase* markers and the basal keratinocyte marker Δ*Np63* (Fig. 2). In the majority of analyzed embryos, clones of labeled cells solely consisting of four to eight ΔNp63-positive but *ATPase*-negative keratinocytes were obtained (data not shown). However, we also identified several embryos in which the clone of labeled descendents consisted of a single *ATPase*-positive and ΔNp63-negative ionocyte, and up to six keratinocytes (Fig. 2). It is noteworthy that no clones with two neighboring ionocytes were found. These data indicate that progenitor cells of the ventral ectoderm give rise to both ionocytes and keratinocytes, and that ionocytes are segregated from a pool of keratinocyte precursor cells.

foxi3a and foxi3b are essential for ionocyte differentiation

forkhead box genes comprise a large number of highly conserved transcription factors that have been identified in a variety of species from yeast to humans. Interestingly, mice lacking the *forkhead* box gene *Foxi1*, a close relative of zebrafish *foxi3a* and *foxi3b* described here, suffer from deafness, renal tubular acidosis and defects in epididymal sperm maturation (Blomqvist et al., 2004, 2006; Hulander et al., 2003). Renal and epididymal acidosis result from the absence of intercalated cells in the collecting duct of the kidneys, and narrow and clear cells in the epididymal epithelia. Such cells are special ionocytes involved in acid–base balancing. They express V-type H^+-ATPases (Blomqvist et al., 2004, 2006) similar to the HR skin ionocytes described here.

To further analyze the roles of *foxi3a* and *foxi3b* in HR as well as NaR cells, we carried out gene-specific loss- and gain-of-function experiments by injecting zebrafish embryos with the respective antisense morpholino oligonucleotides (MOs) or synthetic mRNAs. At the used concentrations (0.15 mM), both MOs completely blocked the production of GFP from co-injected *foxi3a-GFP* or *foxi3b-GFP* fusion mRNAs (data not shown), suggesting that they also efficiently inactivate endogenous *foxi3* transcripts. Injection of *foxi3a* MOs resulted in the complete loss of both *atp6v1al*-expressing HR and *atp1b1b*-expressing NaR cells (compare Figs. 3E, F with Figs. 3B, C), indicating that *foxi3a is* absolutely essential for both types of ionocytes. In contrast, knockdown of *foxi3b* led to a complete loss of HR cells, while the number of NaR cells was reduced to approximately 40% (Figs. 3G, H). Together, this indicates that the ventrally restricted HR cells are strictly dependent on both *foxi3a* and *foxi3b*, whereas *foxi3b* plays a less essential role in the slightly earlier differentiating and both dorsally and ventrally positioned NaR cells (see Discussion).

For gain-of-function studies, synthetic *foxi3a* and/or *foxi3b* mRNA was injected into one-cell stage embryos. At 24 hpf, both single- and double-injected embryos displayed normal numbers and normal densities of NaR and HR cells in their natural domains, the ventral trunk and tail in the case of HR cells (Figs. 3K, O; and data not shown), and both ventral and dorsal trunk and tail regions in the case of NaR cells (Figs. 3J, N; and data not shown). However, ectopic HR cells were obtained in the dorsal trunk (Figs. 3K, O). In addition, ectopic NaR and HR cells were present in the head region, which is normally devoid of any ionocytes (compare Figs. 3I, L, M, P with Figs. 3A, D). Also, the density of ectopic head ionocytes was much higher than in the natural ionocyte domains. Together, these data suggest that forced *foxi3* expression is sufficient to induce ionocyte formation at ectopic sites. However, it fails to induce extra ionocytes within their natural domains, indicating that here, mechanisms must be at play to restrict the expansion of the ionocyte lineage (see below).

ΔNp63 has no effect on ionocyte proliferation or differentiation

We have shown above that *foxi3* genes are temporarily co-expressed with Δ*Np63* (Fig. 1). Δ*Np63* is necessary for the proliferation of keratinocytes (Lee and Kimelman, 2002), as evidenced here by an approximately 3-fold reduction in the number of *col1a1*-positive basal epidermal cells (Dubois et al., 2002; Fisher et al., 2003) in Δ*Np63* morphants at 24 hpf (Figs. 3U, V). In contrast, the number of *atp6v1al*- and *atp1b1b*-positive cells was largely unaltered in Δ*Np63* morphants of the same stage (Figs. 3Q, R), suggesting that ΔNp63 has no effect on the proliferation of ionocyte precursors. One explanation for such a differential effect on keratinocyte versus ionocyte precursors could be that the pro-proliferative role of ΔNp63 only becomes important after ionocytes have segregated out and switched off Δ*Np63* expression. Alternatively, it could mean that a possible positive effect of ΔNp63 on ionocyte proliferation, reducing ionocyte numbers in morphants, was compensated by a negative effect on ionocyte specification. The latter effect would result in increased numbers of ionocytes in morphants and would be consistent with the persistent expression of Δ*Np63* in keratinocytes. To look into this possibility, we carried out Δ*Np63* overexpression studies, injecting synthetic Δ*Np63* mRNA. Such embryos displayed normal numbers of *col1a1*-positive basal keratinocytes (data not shown), suggesting that increased ΔNp63 levels have no effect on the proliferation of keratinocyte precursor cells. If the same was true for ionocytes, a negative effect of ΔNp63 on ionocyte specification should lead to a decrease in ionocyte numbers, which would not be hidden by compensatory pro-proliferative effects. However, ionocyte numbers in Δ*Np63* mRNA-injected embryos were normal (Figs. 3S, T) rather than reduced. Together these data suggest that ΔNp63 has no effect on ionocyte proliferation or differentiation despite its transient expression in ionocyte precursors before their segregation from the keratinocyte lineage.

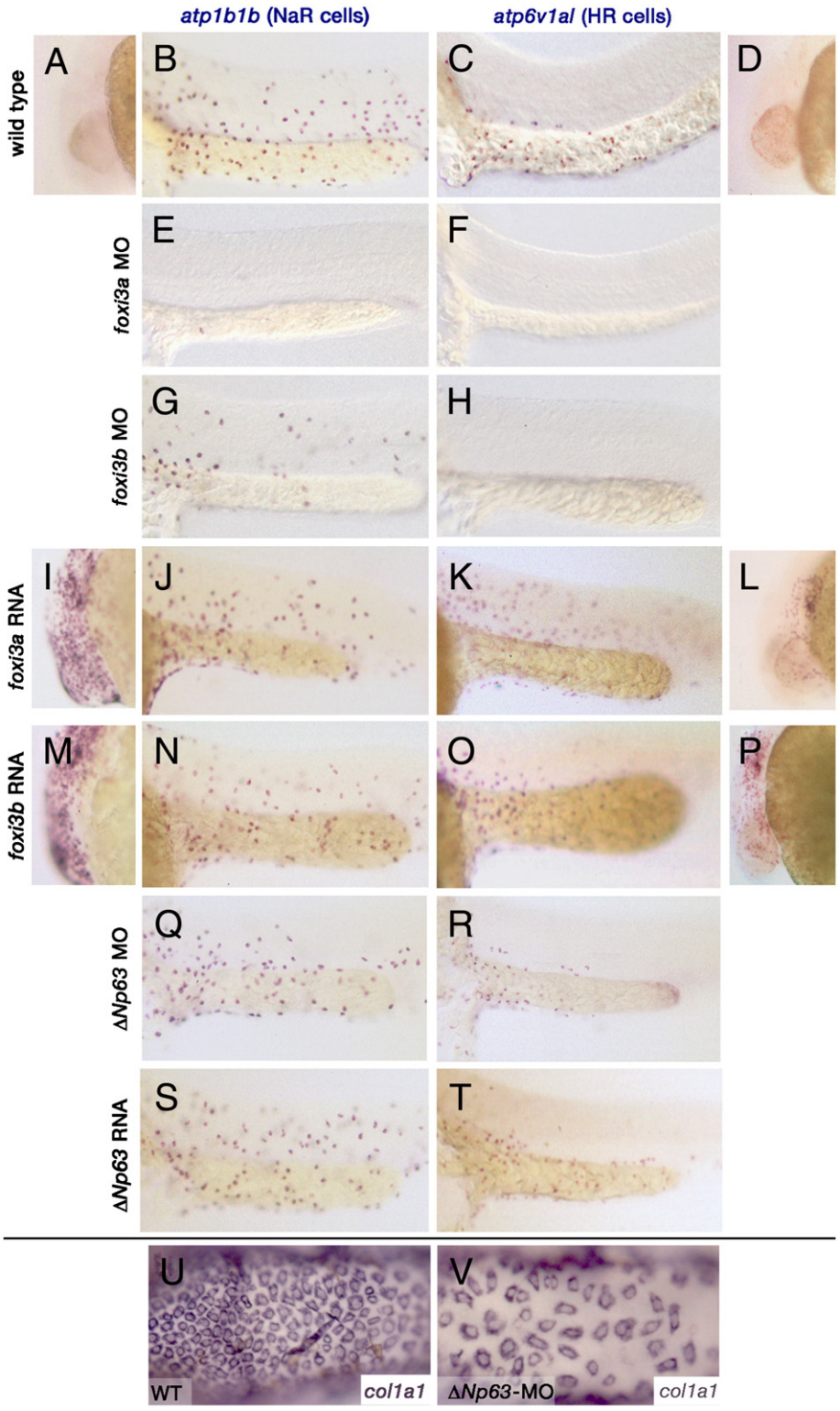

Fig. 3. *foxi3a* and f*oxi3b* are necessary and sufficient for ionocyte differentiation, whereas Δ*Np63* is not involved. All panels show whole-mount in situ hybridizations of embryos at 24 hpf; (A, D, I, L, M, P) show lateral views on head region, (U, V) dorsal views on head regions and all other panels lateral views on the trunk at the level of the yolk sac extension; anterior is always to the left. Probes used were *atp1b1b* staining NaR cells (left column; A, B, E, G, I, J, M, N, Q, S), *atp6v1al* staining HR cells (right column; C, D, F, H, K, L, O, P, R, T) or *col1a1* staining basal keratinocytes (U, V). The nature of embryos is indicated on the left side of each row (A–T) or in the lower left corners of the panels (U, V). (A–D, U) uninjected wild-type controls; (E, F) *foxi3a* morphants; (G, H) *foxi3b* morphants; (I–L) embryos injected with *foxi3a* mRNA; (M–P) embryos injected with *foxi3b* mRNA; (Q, R, V) Δ*Np63* morphants; (S, T) embryos injected with Δ*Np63α* mRNA.

Ionocyte cell numbers and density are regulated by Notch signaling

Differential cell fate decisions among neighboring cells are often controlled by mechanisms of lateral inhibition, mediated by Delta/Jagged–Notch signaling (Lewis, 1998). As a general concept, cells singled out from an epithelium to adapt a particular fate express transmembrane ligands of the Delta/Jagged family, which bind to and activate Notch transmembrane receptors in adjacent cells. In these neighbors, activated Notch is proteolytically cleaved, followed by the release of its intracellular domain (Notch-ICD) from the membrane and the translocation of Notch-ICD into the nucleus, where it converts transcriptional repressor complexes into activators. This leads to the transcriptional activation of members of the *hairy/enhancer-of-split* (*her*) gene family, which encode transcription factors that in turn repress genes activated in the Delta/Jagged cell.

The distribution of single ionocytes within a layer of keratinocytes suggests that Delta/Jagged–Notch signaling could also be involved in the differentiation of these cells. We therefore analyzed ionocyte numbers and distribution in *mind-bomb* (*mib*) mutants, which fail to signal through the Delta/Jagged–Notch pathway due to the absence of a Delta/Jagged-ubiquitin ligase (Itoh et al., 2003). At the 5-somite stage, large clusters of *foxi3a* or *foxi3b*-positive ionocyte precursors were visible in the yolk sac epidermis of *mib* mutants, which was in striking contrast to the even distribution of single cells in wild-type siblings (Figs. 4A–D). At 24 hpf, numbers of both the *atp1b1b*-positive NaR cells and the *atp6v1al*-positive cells were significantly increased in *mib* mutants, with an approximately 50% increase in the case of NaR cells (Figs. 4E, G and 5A), and an even 250% increase in the case of HR cells (Figs. 4F, H and 5A). However, in contrast to the clustered organization of ionocyte precursors at the 5-somite stage (Figs. 4C, D), ionocytes in *mib* mutants at 24 hpf displayed rather equal spacing between individual cells despite their increased density (Figs. 4G, H).

For gain of Notch signaling, we took advantage of the *hsp70:Gal4* and *UAS:notch1a-icd* transgenic lines (Scheer and Campos-Ortega, 1999) to force expression of the constitutively active *notch-icd* by raising the incubation temperature. Two fish heterozygous for the *hsp70:Gal4* or *UAS:notch1a-icd* transgene, respectively, were mated, resulting in double-transgenic embryos in 25% of the offspring. To activate ubiquitous *notch-icd* expression, offspring were heat-shocked for 30 min at various time points during segmentation. While single transgenics or wild-type siblings were unaffected by the heat shock at any time, double transgenic embryos displayed a complete loss of both NaR and HR cells when heat-shocked between the 11- and 23-somite stage (Figs. 4I, J). However, upon forced expression of *notch-icd* at the 25-somite or a later stage, ionocytes remained at normal numbers (data not shown).

Together, these data suggest that constitutively active Notch signaling within ionocyte precursors during early segmentation stages can suppress ionocyte differentiation, while its loss leads to an expansion of the ionocyte lineage. This expansion most likely occurs at the expense of keratinocytes, as at 24 hpf, numbers of ΔNp63-positive cells in *mib* mutants had decreased to approximately 95% of wild-type levels in dorsal regions (which only harbor NaR cells) and to 85% in ventral regions (which harbor NaR and HR cells).

As a first step to study which particular Notch and Delta/Jagged proteins might be involved in this process, we analyzed the expression of the different *delta* and *jagged* genes. Expression of *notch1a has* been reported in the developing neural plate (Bierkamp and Campos-Ortega, 1993). During the early stages of somitogenesis we found *notch1a* ubiquitously expressed throughout the whole embryo (data not shown). In contrast to the Notch receptors, which should be present throughout the entire epithelium, Notch ligands should only be expressed in ionocyte precursors. Indeed, *jagged1a*, *jagged1b* (Zecchin et al., 2005) and *deltaC* (Haddon et al., 1998) were weakly expressed in a punctate pattern at both the 5-somite and 11-somite stage (Fig. 5B, and data not shown), while *jagged 2a* (Zecchin et al., 2005, 2007) showed prominent punctate expression in the epidermis at the 11-somite stage (Fig. 5C). In contrast, no expression was detected for *deltaA*, *deltaB* and *deltaD* (Haddon et al., 1998) (data not shown). In addition to these previously described Notch ligands, we found a second *jagged2* gene, named *jagged2b* (XM_689725), in the GenBank database. *jagged2b* was also weakly expressed in a punctate pattern at the 11-somite stage (Fig 5D). Double in situ hybridization further showed that *jagged2a* is co-expressed with *foxi3a* and *foxi3b* (Figs. 5E, F), indicating that it is particularly activated in ionocyte precursors.

Next, we investigated ionocyte formation upon inactivation of particular *notch*, *delta* or *jagged* genes. Currently, zebrafish mutants in three Notch pathway members have been identified, *bea* (*delta C*) (Julich et al., 2005), *aei* (*delta D*) (Holley et al., 2000) and *des* (*notch 1a*) (Gray et al., 2001). While no alterations were found in *deltaC* and *deltaD* mutants at 24 hpf (data not shown), *notch1a* mutants displayed a more than 100% increase in the number of HR cells, and a 40% increase in the number of NaR cells (Figs. 5A, G, H; and data not shown). This effect, however, was weaker than that obtained for *mib* mutants, in which signaling via all Notch receptors is blocked (Fig. 5A), suggesting that Notch1a plays an essential but partially redundant role in restricting ionocyte specification. To block Jagged function, we injected antisense MOs specifically blocking translation or splicing of *jagged1a*, *jagged1b*, *jagged2a* or *jagged2b* mRNAs (see Materials and methods). However, no alterations in the numbers of *atp1b1b*- or *atp6v1al*-positive ionocytes were detected at 24 hpf even upon quadruple knockdown, co-injecting MOs against all four *jagged* genes (data not shown).

Notch signaling blocks ionocyte specification by repressing foxi3 and other thus far unidentified factors

The data described thus far indicate that *foxi3a* and *foxi3b* are required for ionocyte specification, while Notch ligands made by ionocyte precursors block the same fate in neighboring

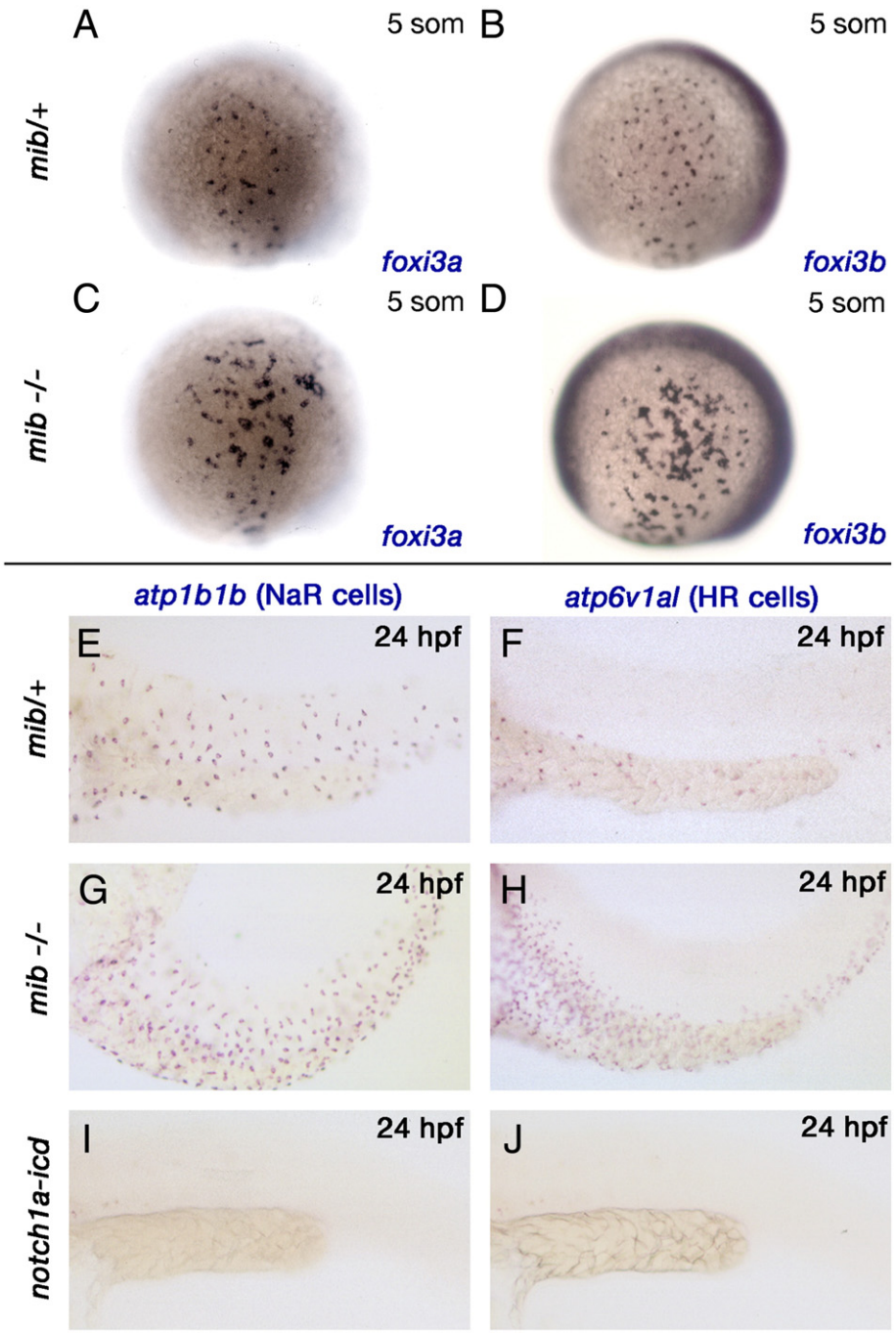

Fig. 4. Notch signaling blocks ionocyte fates. All panels show whole-mount in situ hybridizations of embryos at stages indicated in the top right corners. Genotypes of embryos are indicated on the left side of rows. Probes used were *foxi3a* and *foxi3b* staining ionocyte precursors (A–D), *atp1b1b* staining NaR cells (E, G, I) or *atp6v1al* staining HR cells (F, H, J). Panels A–D show lateral views of entire embryos, dorsal side up, anterior to the left. Panels E–J are lateral views of posterior trunk and tail, dorsal side up, anterior to the left.

cells. We next wanted to investigate whether ionocytic Foxi3 proteins induce lateral inhibition by transcriptional activation of Notch ligand genes, and whether in neighboring cells, this effect is mediated via a transcriptional repression of *foxi3* expression by Notch signaling.

To address the first question, we carried out *jagged2a* in situ hybridizations upon loss of *foxi3* activity. Indeed, *foxi3a* and *foxi3b* morphants lacked epidermal *jagged2a* expression at the 11-somite stage (Figs. 6A, B; compare with Fig. 5C as control), suggesting that Foxi3 is required to initiate or maintain *jagged2a* expression in ionocyte precursors. This is consistent with the absence of the normally punctate expression of *Jagged1* in the inner ear endolymphatic duct/sac epithelium of *Foxi1* mutant mice (Hulander et al., 2003).

To address the second question, we performed various combined Foxi3 and Notch gain- and loss-of-function experiments. First, we generated double deficient embryos, injecting *foxi3a* MOs into *mib* mutants. At 24 hpf, these embryos lacked

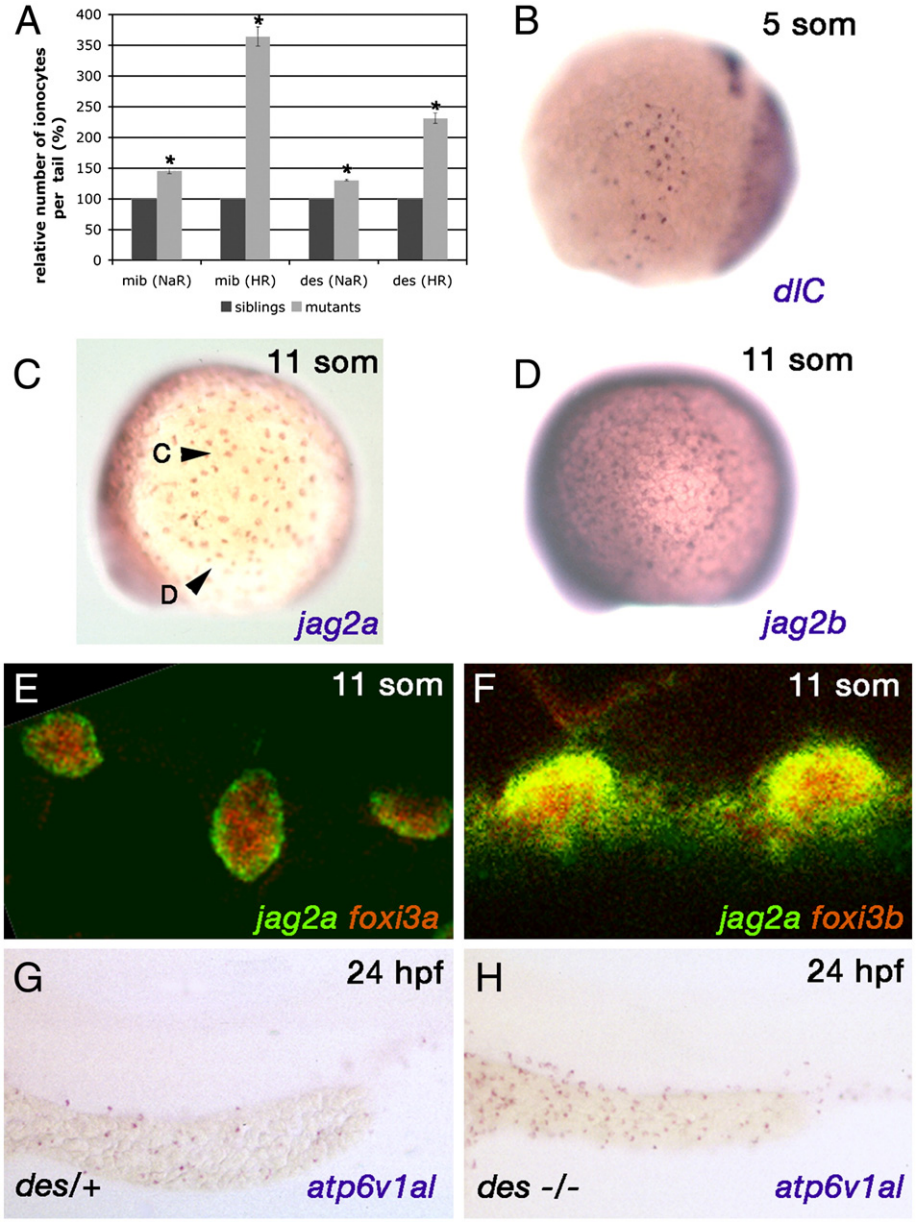

Fig. 5. Ionocyte precursors display expression of *deltaC* and *jagged* genes and are expanded in *notch1a* mutants. (A) Graphical illustration of relative numbers of *atp1b1b*-positive NaR cells and *atp6v1al*-positive HR cells in *mib* mutants lacking entire Notch signaling, and in *des* mutants lacking the Notch1a receptor. Ionocytes were counted on the left side of the trunk and tail of 24 hpf embryos from the anterior start of the yolk sac extension through the tip of the tail. Total numbers were determined for 5 mutants and 5 wild-type siblings (see Figs. 4E–H and Figs. 5G, H for representative examples). Numbers are presented as the quotient of mutant versus wild-type values (grey bars), with wild-type set to 100% (black bars). Asterisks indicate significance beyond the 0.005 level, using Student's *t* test. Panels B–H show whole-mount in situ hybridization of embryos at stages indicated in top right corners and probes indicated in bottom right corners; (B, C, D, G, H) single colorimetric hybridization; (E, F) double fluorescent hybridization. (B–D) Wild-type embryo at 5-somite stage displaying single *deltaC*-positive ectodermal cells (B), and wild-type embryos at 11-somite stage, displaying *jagged 2a*- (C) and *jagged 2b*-positive cells (D) over the yolk sac; dorsal side up, anterior to the left. (E, F) High magnification views on *jagged2a*, *foxi3*-double positive ionocyte precursors on the yolk sac of wild-type embryos at the 11-somite stage, at positions as indicated in panel C. (G–H) Lateral views on posterior trunk and tail of *des* (*notch1a*) mutant (G) and wild-type sibling (H) at 24 hpf, revealing a significant increase in the number of HR cells in the mutant; dorsal side up, anterior to the left.

both NaR and HR ionocytes like regular *foxi3a* morphants (Figs. 6C, D; compare with Figs. 3E, F and 4G, H). In genetic terms, this indicates that Foxi3 is epistatic to Notch signaling, suggesting that Notch signaling restricts the expansion of the ionocyte lineage by blocking *foxi3* expression in neighboring cells. If this was the only mechanism of Notch action, re-introduction of Foxi3 should compensate for up-regulated Notch signaling. However, this was not the case. Instead, injection of *foxi3a* or *foxi3b* mRNA, or co-injection of both, into heat-shocked *hsp70:Gal4*; *UAS:notch1a-icd* double transgenic embryos did not rescue *atp1b1b* or *atp6v1al* expression on trunk, tail and yolk sac extension (Figs. 6E, F; and data not shown; compare with Figs. 3J, K and 4I, J). This suggests that during normal development, Notch signaling blocks ionocyte

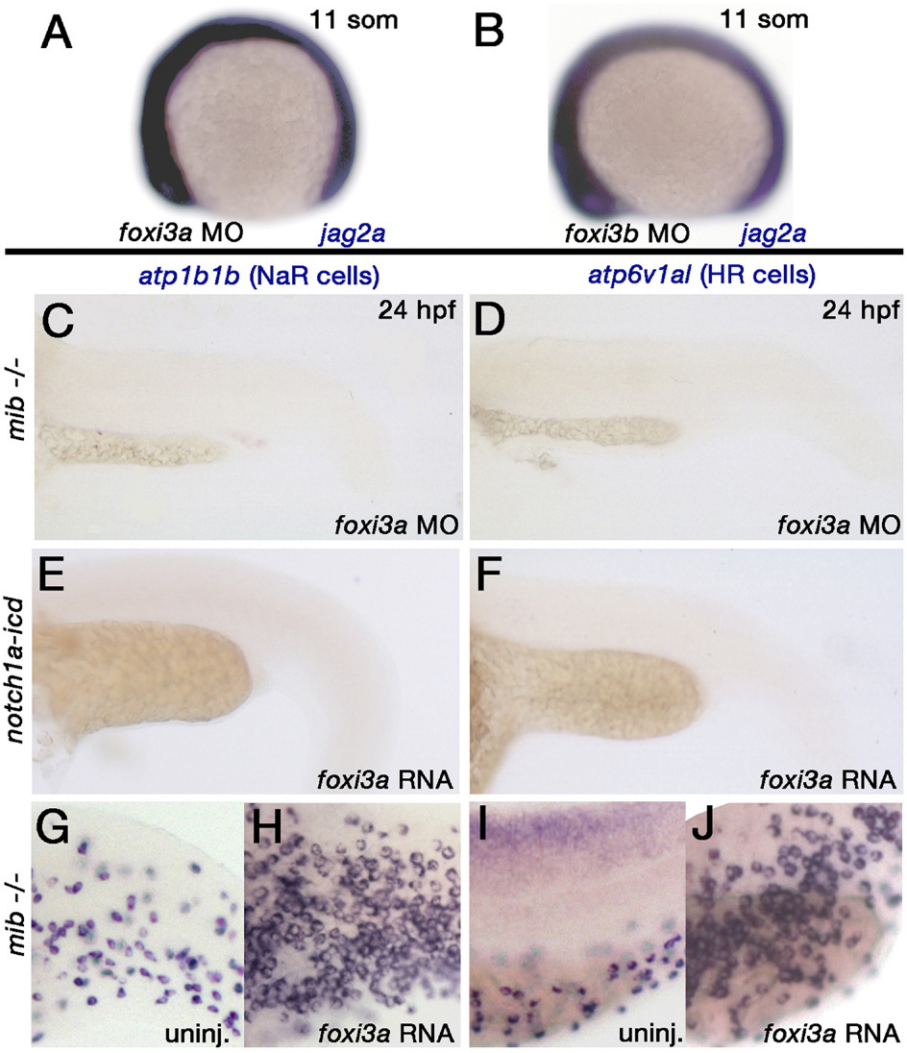

Fig. 6. *jagged2a* expression is dependent on Foxi3, while the anti-ionocyte effect of Notch signaling is achieved by the repression of *foxi3* and another thus far unidentified partner. (A, B) *jagged2a* in situ hybridization, 11-somite stage, lateral views, anterior at the top, dorsal to the right; (A) *foxi3a* morphant, (B) *foxi3b* morphant, both of which lack *jagged2a* expression on the yolk sac. Embryos were overstained to look for residual *jagged2a* transcripts. For positive control, see Fig. 5C. (C–J) In situ hybridizations for *atp1b1b*, labeling NaR cells (left column; C, E, G, H), and for *atp6v1al*, labeling HR cells (right column; D, F, I, J); 24 hpf, lateral view on trunk and tail (C–F) or higher magnification of tail at the level of the yolk sac extension (I, J) or posterior of it (G, H). (C, D) *mib* mutants injected with *foxi3a* MOs lack ionocytes like regular *foxi3a* morphants (Figs. 3E, F). This indicates that supernumerary ionocytes formed in the absence of Notch signaling (Figs. 4G, H) require Foxi3a function. (E, F) Embryos after injection of *foxi3a* mRNA and activation of Notch ICD lack ionocytes as regular *notch-icd* embryos (Figs. 4I, J). This indicates that Foxi3a is not sufficient to overcome the effect of Notch signaling, and that Foxi3 acts in concert with another factor that is subject to repression by Notch signaling. (G–J) *mib* mutants injected with *foxi3a* mRNA (H, J) display a significant increase in the number of ionocytes compared to uninjected *mib* mutants (G, I), in contrast to the failure of *foxi3a* mRNA to induce supernumerary ionocytes in the natural domains of wild-type embryos (Figs. 3J, K). This indicates that only in the absence of Notch signaling, Foxi3 is sufficient for supernumerary ionocyte induction, providing further evidence for the existence of another factor normally repressed by Notch signaling that is required for ionocyte specification.

specification by repressing other genes in addition to *foxi3a* and *foxi3b*. Finally, we combined gain of Foxi3 function with loss of Notch signaling, injecting *foxi3* mRNA into *mib* mutants. As described above, wild-type embryos injected with *foxi3* mRNA only displayed ectopic ionocyte formation in domains normally devoid of these cell types, whereas ionocyte numbers and densities in their endogenous domains on trunk, tail and yolk sac remained unaltered (Figs. 3I–P). Upon injection into *mib* mutants, however, the number of *atp1b1b*- and *atp6v1al*- positive cells in their natural domains was several-fold increased compared to uninjected *mib* mutants (Figs. 6G–J). Strikingly, under these conditions, many ionocytes were positioned right next to another, rather than being separated by keratinocytes. This indicates that only in the absence of Notch signaling, Foxi3 is sufficient to induce supernumerary ionocytes in the natural ionocyte domains, again pointing to the presence of additional factors normally blocked by Notch signaling that are required for ionocyte specification in addition to Foxi3.

Discussion

Ionocytes can be found in several vertebrate tissues including the mammalian kidney, the amphibian skin and the skin and gills of teleost fish (reviewed in Brown and Breton,

1996). While their physiological features have been extensively studied in the past decades (Ehrenfeld and Klein, 1997; Jouret et al., 2005; Perry et al., 2003; Satlin and Schwartz, 1987), the mechanisms of their development, including the genetic control system, were largely unknown. Here, performing double labeling with ionocyte and keratinocyte markers in combination with cell lineage tracing studies (Figs. 1 and 2), we have shown that zebrafish skin ionocytes derive from epidermal precursor cells that also give rise to skin keratinocytes. Previous work has revealed that the proliferation of keratinocyte precursors depends on the p53-related transcription factor ΔNp63 (Bakkers et al., 2002; Lee and Kimelman, 2002). However, this does not seem to be the case for ionocytes, as indicated by normal numbers of ionocytes in Δ*Np63* morphant embryos (Fig. 3). This is consistent with our finding that in contrast to keratinocytes, Δ*Np63* expression in ionocyte precursors is switched off during early segmentation stages, shortly after the expression of ionocyte-specific markers has been initiated (Fig. 1). In addition, ΔNp63 does not seem to play a role in blocking ionocyte differentiation, as indicated by the normal expression of ionocyte markers after forced expression of Δ*Np63* (Fig. 3). Instead, we could identify the Forkhead box transcription factors Foxi3a and Foxi3b as essential positive and intrinsic regulators of ionocyte specification. Furthermore, we have shown that Notch signaling suppresses ionocyte fates in neighboring cells that become keratinocytes.

foxi3a and foxi3b are necessary for the differentiation of skin ionocytes

Members of the family of Forkhead box transcription factors have been implicated in multiple cellular processes, including cell-cycle regulation, cellular survival, cell metabolism, immunoregulation and embryonic development (reviewed in Wijchers et al., 2006). In mouse, the forkhead box transcription factor Foxi1 is required for the formation of intercalated cells in the collecting ducts of the kidneys (Blomqvist et al., 2004) and for the formation of narrow and clear cells in the epididymis (Blomqvist et al., 2006). Both cell types constitute specialized ionocytes that highly express vacuolar H^+-ATPase proton pumps and that are required for the regulation of acid–base balance (Blomqvist et al., 2004, 2006). In the zebrafish genome two homologues of the mammalian *foxi1* gene have been identified and annotated as *foxi3a* and *foxi3b* (Solomon et al., 2003). A very recent study showed that depletion of *foxi3a* results in strongly reduced numbers of HR cells, a subtype of ionocytes in the zebrafish skin that also contains V-type H^+-ATPases and that is restricted to ventral regions of the embryo (Esaki et al., 2006).

We have further analyzed the role of both *foxi3a* and *foxi3b* in the differentiation of HR cells and a second known type of ionocytes called NaR cells, which are characterized by the presence of Na^+/K^+-ATPases. In contrast to the ventral restriction of HR cells, NaR cells are evenly distributed throughout the entire skin of trunk, tail and yolk sac of zebrafish embryos. *foxi3a* and *foxi3b* are expressed in NaR as well as HR cells prior to the expression of the ATPase genes and can therefore be used as a marker for ionocyte precursor cells (Fig. 1). Knockdown experiments using MOs showed that *foxi3a* is absolutely required for the differentiation of both ionocyte types, while knockdown of *foxi3b* leads to a loss of HR cells, but only a reduction in the number of NaR cells (Fig. 3). This partial effect of Foxi3b on NaR cells might be correlated with differences within the population of these cells. In fact, it has been reported that a subset of NaR cells expresses a Ca^{2+}-channel in addition to the Na^+/K^+-pump subunit encoded by *atp1b1b* (Pan et al., 2005). In this light, it is tempting to speculate that Foxi3b might only be required for the specification of HR cells and one subtype of NaR cells, whereas Foxi3a is required in all ionocytes. Still, it is remarkable that for HR cells and the other NaR cell type, both Foxi3a and Foxi3b are absolutely essential, indicating that they have non-redundant roles despite their high structural similarities. In early zebrafish embryogenesis, a similar non-redundant role has been reported for the Bone Morphogenetic proteins Bmp2b and Bmp7, secreted growth factors that appear to act as hetero-dimers (Dick et al., 2000; Schmid et al., 2000). Dimerization as a crucial functional step has also been reported for Foxp proteins (Stroud et al., 2006), and it will be interesting to investigate whether similar mechanisms might be at play between Foxi3a and Foxi3b.

The molecular mechanisms downstream of Foxi3 proteins that drive ionocyte differentiation are also unclear. Mouse Foxi1 has been shown to directly activate the transcription of the ATP6V1B1 gene, which encodes the B1-subunit of the vacuolar H^+-ATPase pump (Blomqvist et al., 2006), and the *AE4* gene, which encodes the anion HCO^{3-}/ Cl^- exchanger (Kurth et al., 2006). Therefore, it could be possible that zebrafish Foxi3a and Foxi3b are direct transcriptional activators of *atp1b1b* and *atp6v1a*. Consistent with this notion, we could identify conserved Fox binding sites in the promoter regions of both genes (own unpublished data). If so, however, there must be additional mechanisms to account for the delay of *ATPase* gene expression, which starts approximately 5 h after the onset of *foxi3* activation.

A positive role of Foxi3a and Foxi3b during zebrafish ionocyte specification was also revealed in gain-of-function experiments. Injection of either or both mRNAs into embryos at the one-cell stage led to the formation of ectopic NaR and HR cells in the head region, which are normally devoid of ionocytes (Fig. 3). However, this treatment did not affect the number or density of ionocytes within their natural domains in trunk, tail or yolk sac. This suggests that in contrast to the head, specific mechanisms exist in these natural domains that restrict the ionocyte lineage and render the majority of the common ionocyte-keratinocyte precursor cells incompetent for Foxi3 proteins.

Notch signaling restricts ionocyte lineage by repressing foxi3 and other thus far unidentified essential positive regulators of ionocyte specification

Our data have identified Notch signaling as the system restricting the ionocyte lineage in the zebrafish skin, in line

with its function in lateral inhibition and singling out of particular cell types from a sheet of precursor cells in many other processes during invertebrate and vertebrate development (Lewis, 1998). Shortly after the onset of *foxi3* expression, zebrafish ionocyte precursors display expression of the Notch ligands Jagged2a and, to a lower extent, DeltaC, Jagged1a, Jagged1b and Jagged2b (Fig. 5 and data not shown). This expression seems to depend on Foxi3 function since *jagged2a* expression is absent in ionocyte precursors of *foxi3* morphants (Fig. 6). However, it remains unclear whether Foxi3 is required for the initiation or the maintenance of *Jagged* expression (see also below and Fig. 7). Our data from mutant analyses and antisense morpholino oligonucleotide injections indicate that DeltaC and the four Jagged ligands are dispensable for proper ionocyte spacing. Even concomitant inactivation of all four Jagged proteins did not alter the number of differentiated ionocytes, ruling out functional redundancy among the paralogues. However, we want to point out that while this article was in revision, Hsiao et al. (2007) published that the number of *foxi3*-positive ionocyte precursors is increased in *deltaC* mutants of the tailbud stage. They suggest that DeltaC is the only ligand mediating lateral inhibition during ionocyte differentiation. However, as mentioned above, we could not detect any differences in the number of differentiated, ATPase-positive ionocytes in older *deltaC* mutants (24 hpf). This suggests that DeltaC is only required for blocking early steps of ionocyte segregation, whereas blockage of later steps of ionocyte differentiation and/or during later phases of lineage expansion (see below) is mediated by other or additional Notch ligands, possibly Jaggeds. Further experiments will be necessary to resolve this issue.

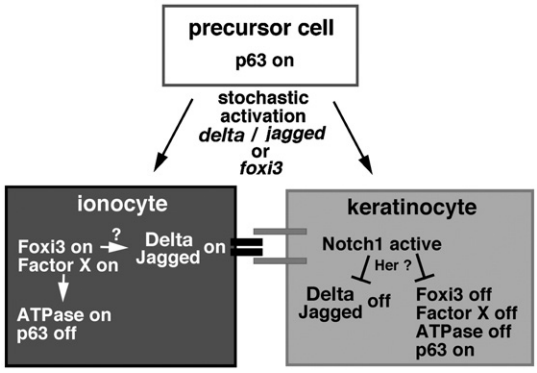

Fig. 7. Model for ionocytes versus keratinocyte specification. Ionocytes and keratinocytes derive from a common pool of epidermal precursor cells characterized by the expression of the transcription factor ΔNp63 (white box). *foxi3a* and *foxi3b* are activated in individual precursor cells, followed by *delta*/*jagged* expression (black box). Delta/Jagged, in turn, induces lateral inhibition by signaling to neighboring cells, where activated Notch signaling leads to a repression of *foxi3a*, *foxi3b* and *delta*/*jagged* expression (grey box). This repression might be mediated by *her* genes, which in many other instances have been shown to be activated by Notch signaling, encoding transcriptional repressors of genes required for the fates of Delta/Jagged cells (Lewis, 1998). Once stable expression levels have been established, Foxi3 proteins lead to ionocyte specification, characterized by the loss of Δ*Np63* expression and the transcriptional activation of *ATPase* genes. Future experiments have to reveal whether Foxi3 proteins are direct activators of *ATPase* genes. Foxi3-negative neighbors of ionocytes, however, differentiate into keratinocytes, characterized by maintained Δ*Np63* expression and the initiation of *col1a1* expression, while *ATPase* genes remain non-transcribed. It remains to be shown whether Foxi3 is the stochastically regulated trigger, with Foxi3 initiating *delta*/*jagged* expression, or whether Foxi3 is only required for the maintenance of *delta*/*jagged* expression (indicated by question mark in black box), while *delta*/*jagged* initiation is subject to the stochastic mechanism, with *foxi3* being constitutively activated unless repressed by Notch. Furthermore, our Foxi3–Notch epistasis analyses point to the existence of the thus far unidentified factor X which appears to act as a partner of Foxi3 during ionocyte differentiation, while it is repressed by Notch signaling in future keratinocytes.

In contrast to our Delta or Jagged loss-of-function experiments, general blockage of Notch signaling in *mib* mutants (Itoh et al., 2003) (Fig. 4) or loss of the Notch1a receptor in *des* mutants (Gray et al., 2001) (Fig. 5) led to a significant increase in the number of both NaR and HR cells at 24 hpf. Already at the 5-somite stage, large cluster of ionocyte precursor cells were detected in *mib* mutants, whereas in siblings, progenitors were distributed as single and equally spaced cells (Fig. 4). This strongly suggests that Notch signaling constitutes a system of lateral inhibition to block ionocyte fates in neighboring cells, which will become keratinocytes. Still, it is interesting to note that despite their increased numbers, ionocytes at 24 hpf display a rather uniform single cell distribution, suggesting that additional mechanisms are at play to secondarily space individual ionocytes.

In contrast to loss of Notch signaling, forced ubiquitous expression of the constitutively active intracellular Notch domain (Notch-ICD) resulted in a loss of all ionocytes (Fig. 4). This effect was achieved when *notch-icd* was activated during mid-segmentation stages, several hours after the initiation of *foxi3* expression. This suggests that in the presence of Notch signaling, Foxi3 is not sufficient to induce ionocyte differentiation. The same conclusion can be drawn from our observations that trunk and tail ionocytes failed to differentiate upon a combination of forced *foxi3* and *notch-icd* expression, whereas forced *foxi3* expression did lead to supernumerary ionocytes in these natural domains when Notch signaling was blocked (Fig. 6). Together, these results point to the existence of another thus far unidentified factor that is required for ionocyte differentiation and that is subject to repression by Notch signaling in neighboring cells. Negative regulation by Notch signaling also applies to the *foxi3* genes themselves, as indicated by our Notch–Foxi3 epistasis analysis, showing that in the absence of Foxi3 function, loss of (inhibiting) Notch signaling has no further consequences on ionocyte development (Fig. 6). In summary, it appears that ionocyte differentiation requires both Foxi3 and another as yet unidentified factor X, both of which are repressed by Notch signaling in neighboring presumptive keratinocytes (see Fig. 7 for illustration).

A model for pattern formation and ionocytes differentiation in the zebrafish skin

An important open question is how the punctate expression of *foxi3*, factor X and Notch ligand genes in single epidermal precursor cells is initiated. According to current models of lateral inhibition, it could be a plain stochastic effect. Within a

field of undifferentiated precursors, all cells express Notch receptors but compete for the expression of *Notch* ligands (Lewis, 1998). The cell that synthesizes more ligand induces Notch activation and increased *Notch* expression in the neighboring cells, where Notch signaling in turn represses ligand expression. Thereby the cells expressing the ligand will differentiate into one cell type, in our case ionocytes, while the cells expressing the receptor will differentiate into a second cell type, in our case keratinocytes. The absence of *jagged2* expression in *foxi3* morphants (Fig. 6) suggests that Jagged is a transcriptional target and acts downstream of Foxi3, consistent with data obtained for their homologues Jagged1 and Foxi1 in the inner ear of the mouse (Hulander et al., 2003), and consistent with the presence of consensus Fox binding sites in the zebrafish *jagged2a* promoter region (own unpublished observations). This could mean that rather than *jagged* and/or *delta* genes, the expression of *foxi3* is the stochastically regulated trigger to set up the initial salt-and-pepper pattern, while Jagged–Notch signaling acts in a second step to avoid *foxi3* expression in neighboring cells. Still, with such a strict Foxi3–Jagged epistasis, it would be difficult to explain why in contrast to the head region, forced early expression of Foxi3 did not lead to supernumerary ionocytes in their natural domains (Fig. 3). These findings would be more in line with a lateral inhibition mechanism that is set up in parallel rather than downstream of Foxi3. Such an independently set up Notch system would render the trunk and tail insensitive for forced *foxi3* expression, whereas the strong response in the head region would indicate that here, the Notch system remains inactive, consistent with the restricted expression of *delta* and *jagged* genes. In any case, once stable differential Jagged and Foxi3 levels have been established, Δ*Np63* gene expression is lost and *ATPase* gene expression activated in ionocyte precursors, possibly again mediated by Foxi3 itself (see above). In contrast, in keratinocyte precursors, ΔNp63 expression is maintained, taking care of proper expansion of the keratinocyte lineage.

But how does the ionocyte lineage expand? We think that the singling out of ionocyte precursors is a continuous process that can occur whenever and wherever a cluster of epidermal cells is present that lacks ionocytes and therefore Notch mediated lateral inhibition. Consistent with this notion, we found that the skin of mid-segmentation stage embryos contains ionocytes of different developmental stages, with *foxi3*-positive cells that still contain or have already lost ΔNp63 protein at the 3- and the 17-somite stage, and with ATPase-positive cells that have or have not switched of *foxi3* expression at 24 hpf (Fig. 1). Over time, this consecutive segregation from the pool of epidermal cells leads to increasing numbers and densities of skin ionocytes, until a critical distance between individual ionocytes is reached. It could also account for the recruitment of new ionocytes during skin growth, when keratinocyte proliferation leads to higher inter-ionocyte spacing. However, we want to point out that this later aspect is less relevant, because during the first 5 days of zebrafish development, the total surface of the embryo is only increased 2- to 3-fold, largely caused by changes in the shape of the animal, whereas real volume increase only occurs after the fish has started to take up external food. During these larval stages, however, skin ionocytes are lost and replaced by ionocytes in the gills. The mechanisms underlying this switch are not understood at all.

Acknowledgments

We thank Andrew Oates for kindly providing the *des* mutant line as well as fixed embryos of *aei*, *bea* and *des* mutants, Alexander Reugels for the transgenic lines *UAS:notch1a-icd* and *hsp70:Gal4*, Jacek Topczewski and Lilianna Solnica-Krezel for the *β-actin:mGFP* transgenic line and the Zebrafish International Resource Center (ZIRC) for plasmids. We are also very grateful to Chung-Der Hsiao, Yun-Jin Jiang and Hwang Pung-Pung for exchanging unpublished data, to Donatus Boensch and his team for excellent fish care, to Carina Kramer for help with microinjections and to Petra Kindle for help with confocal microscopy. M.J. is a member of the Graduiertenkolleg GRK 1104 of the University of Freiburg. Work in the laboratory of M.H. was supported by the Max-Planck Society, the National Institute of Health (NIH grant 1R01-GM63904) and the European Union (6th framework integrated project "Zebrafish models for human development and disease").

References

Bakkers, J., Hild, M., Kramer, C., Furutani-Seiki, M., Hammerschmidt, M., 2002. Zebrafish DeltaNp63 is a direct target of Bmp signaling and encodes a transcriptional repressor blocking neural specification in the ventral ectoderm. Dev. Cell 2, 617–627.

Bakkers, J., Camacho-Carvajal, M., Nowak, M., Kramer, C., Danger, B., Hammerschmidt, M., 2005. Destabilization of DeltaNp63alpha by Nedd4-mediated ubiquitination and Ubc9-mediated sumoylation, and its implications on dorsoventral patterning of the zebrafish embryo. Cell Cycle 4, 790–800.

Bierkamp, C., Campos-Ortega, J.A., 1993. A zebrafish homologue of the *Drosophila* neurogenic gene Notch and its pattern of transcription during early embryogenesis. Mech. Dev. 43, 87–100.

Blomqvist, S.R., Vidarsson, H., Fitzgerald, S., Johansson, B.R., Ollerstam, A., Brown, R., Persson, A.E., Bergstrom, G.G., Enerback, S., 2004. Distal renal tubular acidosis in mice that lack the forkhead transcription factor Foxi1. J. Clin. Invest. 113, 1560–1570.

Blomqvist, S.R., Vidarsson, H., Soder, O., Enerback, S., 2006. Epididymal expression of the forkhead transcription factor Foxi1 is required for male fertility. EMBO J. 25, 4131–4141.

Boisen, A.M., Amstrup, J., Novak, I., Grosell, M., 2003. Sodium and chloride transport in soft water and hard water acclimated zebrafish (*Danio rerio*). Biochim. Biophys. Acta 1618, 207–218.

Brown, D., Breton, S., 1996. Mitochondria-rich, proton-secreting epithelial cells. J. Exp. Biol. 199, 2345–2358.

Claiborne, J.B., Edwards, S.L., Morrison-Shetlar, A.I., 2002. Acid–base regulation in fishes: cellular and molecular mechanisms. J. Exp. Zool. 293, 302–319.

Clay, H., Ramkrishnan, L., 2005. Multiplex fluorescent in situ hybridization in zebrafish embryos using tyramide signal amplification. Zebrafish 2, 105–111.

Cooper, M.S., Szeto, D.P., Sommers-Herivel, G., Topczewski, J., Solnica-Krezel, L., Kang, H.-C., Hohnson, I., Kimelman, D., 2005. Visualizing morphogenesis in transgenic zebrafish using BODIYP TR methyl ester dye as a vital counterstain for GFP. Dev. Dyn. 232, 359–368.

Dick, A., Hild, M., Bauer, H., Imai, Y., Maifeld, H., Schier, A., Talbot, W., Bowemeester, T., Hammerschmidt, M., 2000. Essential role of Bmp7 (snailhouse) and its prodomain in dorsoventral patterning of the zebrafish embryo. Development 127, 343–354.

Dubois, G.M., Haftek, Z., Crozet, C., Garrone, R., Le Guellec, D., 2002. Structure and spatio temporal expression of the full length DNA complementary to RNA coding for alpha2 type I collagen of zebrafish. Gene 294, 55–65.

Ehrenfeld, J., Klein, U., 1997. The key role of the H+ V-ATPase in acid–base balance and Na+ transport processes in frog skin. J. Exp. Biol. 200, 247–256.

Esaki, M., Hoshijima, K., Kobayashi, S., Fukuda, H., Kawakami, K., Hirose, S., 2006. Visualization in zebrafish larvae of Na+ uptake in mitochondrion-rich cells whose differentiation is dependent on foxi3{alpha}. Am. J. Physiol., Regul. Integr. Comp. Physiol. 31, 31.

Fisher, S., Jagadeeswaran, P., Halpern, M.E., 2003. Radiographic analysis of zebrafish skeletal defects. Dev. Biol. 264, 64–76.

Goss, G.G., Perry, S.F., Wood, C.M., Laurent, P., 1992. Mechanisms of ion and acid–base regulation at the gills of freshwater fish. J. Exp. Zool. 263, 143–159.

Gray, M., Moens, C.B., Amacher, S.L., Eisen, J.S., Beattie, C.E., 2001. Zebrafish deadly seven functions in neurogenesis. Dev. Biol. 237, 306–323.

Haddon, C., Smithers, L., Schneider-Maunoury, S., Coche, T., Henrique, D., Lewis, J., 1998. Multiple delta genes and lateral inhibition in zebrafish primary neurogenesis. Development 125, 359–370.

Hammerschmidt, M., Pelegri, F., Mullins, M.C., Kane, D.A., van Eeden, F.J., Granato, M., Brand, M., Furutani-Seiki, M., Haffter, P., Heisenberg, C.P., Jiang, Y.J., Kelsh, R.N., Odenthal, J., Warga, R.M., Nusslein-Volhard, C., 1996. dino and mercedes, two genes regulating dorsal development in the zebrafish embryo. Development 123, 95–102.

Holley, S.A., Geisler, R., Nusslein-Volhard, C., 2000. Control of her1 expression during zebrafish somitogenesis by a delta-dependent oscillator and an independent wave-front activity. Genes Dev. 14, 1678–1690.

Hsiao, C.-D., You, M.-S., Guh, Y.-J., Ma, M., Jiang, Y.-J., Hwang, P.-P., 2007. A positive regulatory loop between foxi3a and foxi3b is essential for specification and differentiation of zebrafish epidermal ionocytes. PLoS ONE 2, e302.

Hulander, M., Kiernan, A.E., Blomqvist, S.R., Carlsson, P., Samuelsson, E.J., Johansson, B.R., Steel, K.P., Enerback, S., 2003. Lack of pendrin expression leads to deafness and expansion of the endolymphatic compartment in inner ears of Foxi1 null mutant mice. Development 130, 2013–2025.

Itoh, M., Kim, C.H., Palardy, G., Oda, T., Jiang, Y.J., Maust, D., Yeo, S.Y., Lorick, K., Wright, G.J., Ariza-McNaughton, L., Weissman, A.M., Lewis, J., Chandrasekharappa, S.C., Chitnis, A.B., 2003. Mind bomb is a ubiquitin ligase that is essential for efficient activation of Notch signaling by Delta. Dev. Cell 4, 67–82.

Jouret, F., Auzanneau, C., Debaix, H., Wada, G.H., Pretto, C., Marbaix, E., Karet, F.E., Courtoy, P.J., Devuyst, O., 2005. Ubiquitous and kidney-specific subunits of vacuolar H+-ATPase are differentially expressed during nephrogenesis. J. Am. Soc. Nephrol. 16, 3235–3246.

Julich, D., Hwee Lim, C., Round, J., Nicolaije, C., Schroeder, J., Davies, A., Geisler, R., Lewis, J., Jiang, Y.J., Holley, S.A., 2005. beamter/deltaC and the role of Notch ligands in the zebrafish somite segmentation, hindbrain neurogenesis and hypochord differentiation. Dev. Biol. 286, 391–404.

Kimmel, C.B., Warga, R.M., Schilling, T.F., 1990. Origin and organization of the zebrafish fate map. Development 108, 581–594.

Kurth, I., Hentschke, M., Hentschke, S., Borgmeyer, U., Gal, A., Hubner, C.A., 2006. The forkhead transcription factor Foxi1 directly activates the AE4 promoter. Biochem. J. 393, 277–283.

Lorent, K., Yeo, S.Y., Oda, T., Chandrasekharappa, S., Chitnis, A., Matthews, P.R., Pack, M., 2004. Inhibition of Jagged-mediated Notch signaling disrupts zebrafish biliary development and generates multi-organ defects compatible with an Alagille syndrome phenocopy. Development 121, 5753–5766.

Lee, H., Kimelman, D., 2002. A dominant-negative form of p63 is required for epidermal proliferation in zebrafish. Dev. Cell 2, 607–616.

Le Guellec, D., Morvan-Dubois, G., Sire, J.Y., 2004. Skin development in bony fish with particular emphasis on collagen deposition in the dermis of the zebrafish (*Danio rerio*). Int. J. Dev. Biol. 48, 217–231.

Lewis, J., 1998. Notch signalling and the control of cell fate choices in vertebrates. Semin. Cell Dev. Biol. 9, 583–589.

Lin, L.Y., Horng, J.L., Kunkel, J.G., Hwang, P.P., 2006. Proton pump-rich cell secretes acid in skin of zebrafish larvae. Am. J. Physiol., Cell Physiol. 290, C371–C378.

Nasevicius, A., Ekker, S.C., 2000. Effective targeted gene 'knockdown' in zebrafish. Nat. Genet. 26, 216–220.

Pan, T.C., Liao, B.K., Huang, C.J., Lin, L.Y., Hwang, P.P., 2005. Epithelial Ca(2+) channel expression and Ca(2+) uptake in developing zebrafish. Am. J. Physiol., Regul. Integr. Comp. Physiol. 289, R1202–R1211.

Perry, S.F., Shahsavarani, A., Georgalis, T., Bayaa, M., Furimsky, M., Thomas, S.L., 2003. Channels, pumps, and exchangers in the gill and kidney of freshwater fishes: their role in ionic and acid–base regulation. J. Exp. Zool. A Comp. Exp. Biol. 300, 53–62.

Satlin, L.M., Schwartz, G.J., 1987. Postnatal maturation of rabbit renal collecting duct: intercalated cell function. Am. J. Physiol. 253, F622–F635.

Scheer, N., Campos-Ortega, J.A., 1999. Use of the Gal4-UAS technique for targeted gene expression in the zebrafish. Mech. Dev. 80, 153–158.

Schmid, B., Fürthauer, M., Conners, S.A., Trout, J., Thisse, B., Thisse, C., Mullins, M.C., 2000. Equivalent genetic roles of bmp7/snailhouse and bmp2b/swirl in dorsoventral pattern formation. Development 127, 957–967.

Solomon, K.S., Logsdon Jr., J.M., Fritz, A., 2003. Expression and phylogenetic analyses of three zebrafish FoxI class genes. Dev. Dyn. 228, 301–307.

Stroud, J.C., Wu, Y., Bates, D.L., Han, A., Nowick, K., Paabo, S., Tong, H., Chen, L., 2006. Structure of the forkhead domain of FOXP2 bound to DNA. Structure 14, 159–166.

Thisse, B., Pflumio, S., Fürthauer, M., Loppin, B., Heyer, V., Degrave, A., Woehl, R., Lux, A., Steffan, T., Charbonnier, X.Q. and Thisse, C. (2001). Expression of the zebrafish genome during embryogenesis (NIH R01 RR15402).

Varsamos, S., Nebel, C., Charmantier, G., 2005. Ontogeny of osmoregulation in postembryonic fish: a review. Comp. Biochem. Physiol., A Mol. Integr. Physiol. 141, 401–429.

Wijchers, P.J., Burbach, J.P., Smidt, M.P., 2006. In control of biology: of mice, men and Foxes. Biochem. J. 397, 233–246.

Zecchin, E., Conigliaro, A., Tiso, N., Argenton, F., Bortolussi, M., 2005. Expression analysis of jagged genes in zebrafish embryos. Dev. Dyn. 233, 638–645.

Zecchin, E., Filippi, A., Biemar, F., Tiso, N., Pauls, S., Ellertsdottir, E., Gnugge, L., Bortolussi, M., Driever, W., Argenton, F., 2007. Distinct delta and jagged genes control sequential segregation of pancreatic cell types from precursor pools in zebrafish. Dev. Biol. 301, 192–204.